PLOS ONE

RESEARCH ARTICLE

The IL-10^{GFP} (VeRT-X) mouse strain is not suitable for the detection of IL-10 production by granulocytes during lung inflammation

Müge Özkan[1], **Yusuf Cem Eskiocak**[2], **Gerhard Wingender**[2,3]*

1 Department of Genome Sciences and Molecular Biotechnology, Izmir International Biomedicine and Genome Institute, Dokuz Eylul University, Balcova/Izmir, Turkey, **2** Izmir Biomedicine and Genome Center (IBG), Balcova/Izmir, Turkey, **3** Department of Biomedicine and Health Technologies, Izmir International Biomedicine and Genome Institute, Dokuz Eylul University, Balcova/Izmir, Turkey

* gerhard.wingender@ibg.edu.tr

Citation: Özkan M, Eskiocak YC, Wingender G (2021) The IL-10^{GFP} (VeRT-X) mouse strain is not suitable for the detection of IL-10 production by granulocytes during lung inflammation. PLoS ONE 16(5): e0247895. https://doi.org/10.1371/journal.pone.0247895

Editor: Lynette Beattie, University of Melbourne (Peter Doherty Institute for Infection and Immunity), AUSTRALIA

Received: February 15, 2021

Accepted: April 27, 2021

Published: May 12, 2021

Peer Review History: PLOS recognizes the benefits of transparency in the peer review process; therefore, we enable the publication of all of the content of peer review and author responses alongside final, published articles. The editorial history of this article is available here: https://doi.org/10.1371/journal.pone.0247895

Data Availability Statement: All relevant data are within the manuscript and its Supporting Information files.

Abstract

The clear and unequivocal identification of immune effector functions is essential to understand immune responses. The cytokine IL-10 is a critical immune regulator and was shown, for example, to limit pathology during various lung diseases. However, the clear identification of IL-10-producing cells is challenging and, therefore, reporter mouse lines were developed to facilitate their detection. Several such reporter lines utilize GFP, including the IL-10^{GFP} (VeRT-X) reporter strain studied here. In line with previous reports, we found that this IL-10^{GFP} line faithfully reports on the IL-10 production of lymphoid cells. However, we show that the IL-10^{GFP} reporter is not suitable to analyse IL-10 production of myeloid cells during inflammation. During inflammation, the autofluorescence of myeloid cells increased to an extent that entirely masked the IL-10-specific GFP-signal. Our data illustrate a general and important technical caveat using GFP-reporter lines for the analysis of myeloid cells and suggest that previous reports on effector functions of myeloid cells using such GFP-based reporters might require re-evaluation.

Introduction

Regulatory cytokines are important players during pulmonary inflammation to limit immunopathology without hampering effective pathogen clearance [1]. The regulatory cytokine IL-10 is involved in various lung diseases, like asthma, allergic airway disease (AAD), chronic obstructive pulmonary disease (COPD), and pulmonary infections [1]. IL-10 producing cells in the lung; FoxP3$^+$ and FoxP3$^-$ regulatory T cells [1], CD8$^+$ T cells [2], B cells, alveolar macrophages (AM) [3], interstitial macrophages (IM) [4], airway and alveolar epithelial cells [1], and airway-associated dendritic cells (DCs) [1] were shown to limit disease pathology. However, due to the low percentage of IL-10$^+$ cells within most cell populations and due to the low intensity of the flow cytometric staining of intracellular IL-10 the clear identification of IL-10 producing cells is challenging [5]. Therefore, various reporter mouse lines were developed to avoid the need for intracellular cytokine staining to identify IL-10 producing cells [6]. The IL-

Funding: This work was funded by grants from the Scientific and Technological Research Council of Turkey (TUBITAK, www.tubitak.gov.tr; #116Z272, GW), the Dokuz Eylul University (Izmir, Turkey; www.deu.edu.tr; #2020.KB.SAG.031, GW), and the European Molecular Biology Organization (EMBO, www.embo.org; IG3073; GW). The funders had no role in study design, data collection and analysis, decision to publish, or preparation of the manuscript.

Competing interests: The authors declare no competing financial interests.

Abbreviations: AAD, allergic airway disease; AM, alveolar macrophage; COPD, chronic obstructive pulmonary disease; DC, dendritic cell; HDM, house dust mite; ICCS, intracellular cytokine staining; ILC, innate lymphoid cell; IM, interstitial macrophages; GFP, green fluorescent protein; LPS, lipopolysaccharide; mLN, mediastinal lymph node.

10^{GFP} (VeRT-X) strain studied here, expresses an (IRES)-enhanced green fluorescent protein (eGFP) fusion protein downstream of the exon 5 of the *il10* gene [7], and was reported to enable the identification of IL-10^{+} lymphoid but also myeloid cells [7]. Several myeloid cells possess an autofluorescence around 525 nm [8], which coincides with the emission maxima of GFP around 530 nm [9]. However, the impact of this myeloid autofluorescence on the detection of GFP-reporter signals has not been fully clarified. Here, using an LPS-induced lung inflammation model, we demonstrate that the autofluorescence of myeloid cells conceals the IL10^{GFP}-specific signal. This was mainly due to a large increase in the myeloid autofluorescence during the inflammation. These data demonstrate that not all GFP-reporter mouse strains are suitable to analyse effector functions of myeloid cells during inflammation.

Results and discussion

Neutrophils were suggested to be the primary source of IL-10 in the lung following *Klebsiella pneumoniae ST258* infection [10]. Furthermore, long-term exposure to house-dust mite (HDM) extracts suppressed allergic airway diseases via the IL-10 production by presumably FoxP3^{+} T cells and alveolar macrophages [3]. In both studies, the 'shift' in the GFP-signal in the experimental IL-10^{GFP} group was compared to either the uninfected IL-10^{GFP} group or the naïve C57BL/6 group as control. When we analysed the IL-10 production during lung inflammation, we noticed that the background signal in the GFP-channel (505 nm—550 nm) of leukocytes from the lung, spleen, or mediastinal lymph node (mLN) was comparable in non-inflamed controls of either C57BL/6 (WT) or IL-10^{GFP} mice (**Fig 1A**). Upon LPS-induced lung inflammation, the GFP-signal clearly increased, in particular in the lungs (**Fig 1B**). Nevertheless, the GFP-signal from WT and IL-10^{GFP} mouse-derived cells remained comparable for the percentage (**Fig 1A and 1B**) or the mean fluorescence intensity (MFI, **Fig 1C**), irrespective of the organ analysed and the inflammatory condition. These data suggest that the GFP-signal detected in the IL-10^{GFP}—derived cells was actually a background signal.

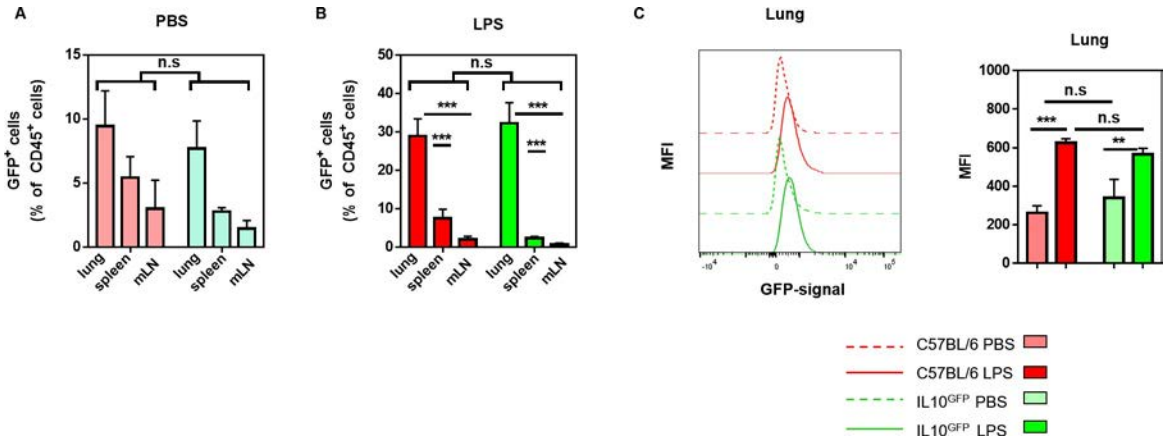

Fig 1. The myeloid-derived GFP signal is comparable between IL10^{GFP} and C57BL/6 mice and increases during lung inflammation. C57BL/6 and IL-10^{GFP} mice were challenged three times (d0, d1, d2) with either PBS or 10 μg LPS per mouse via aspiration. 16–18 hours after the last administration, the single cell suspension from lungs, spleens, and mLNs were stained for CD4^{+} T cells (CD45^{+} CD45R/B220^{-} CD3ε^{+} CD4^{+} CD8α^{-}), CD8^{+} T cells (CD45^{+} CD45R/B220^{-} CD3ε^{+} CD4^{-} CD8α^{+}), macrophages (CD45^{+} CD45R/B220^{-} CD3ε^{-} Siglec-F^{-} F4/80^{+}), Siglec-F^{+} cells (eosinophils, alveolar macrophages; CD45^{+} CD45R/B220^{-} CD3ε^{-} Siglec-F^{+} F4/80$^{-/+}$), neutrophils (CD45^{+} CD45R/B220^{-} CD3ε^{-} Siglec-F^{-} F4/80^{-} Ly6G^{+} CD11b^{+}), monocytes (CD45^{+} CD45R/B220^{-} CD3ε^{-} Siglec-F^{-} F4/80^{-} Ly6G^{-} Ly6C^{+} CD11b^{+}), and ILCs (CD45^{+} CD45R/B220^{-} CD3ε^{-} Siglec-F^{-} F4/80^{-} Ly6G^{-} CD90.2^{+} CD127$^{lo/-}$). The expression of IL-10 was measured either by GFP^{+} or by intracellular IL-10 as indicated. **(A, B)** The frequency of GFP^{+} cells (live CD45^{+}) in the lungs of (A) PBS or (B) LPS challenged C57BL/6 (red) and IL-10^{GFP} (green) mice are shown. The graph shows combined data from three independent experiments (PBS: n = 9 mice/group, LPS: n = 13–15 mice/group in total). **(C)** Representative histogram showing the shift in the GFP-signal (505 nm—550 nm) of live CD45^{+} lung cells upon LPS administration in C57BL/6 and IL-10^{GFP} mice strains.

https://doi.org/10.1371/journal.pone.0247895.g001

To clarify which cell types could produce IL-10, we directly compared the IL-10 signal derived from the GFP-signal or from intracellular cytokine staining (ICCS) for CD4$^+$ and CD8$^+$ T cells, neutrophils, macrophages, Siglec-F$^+$ cells (eosinophils, alveolar macrophages), monocytes, and ILCs. Cells from the lungs, spleens, and mLN of PBS (control) and LPS-challenged C57BL/6 and IL-10^{GFP} mice were analysed (S1 Fig). Although intracellular IL-10 staining is challenging, we obtained a clear IL-10 signal with the commercial antibody (S2 Fig). With this side-by-side comparison, we found that the IL-10-signal derived from GFP or ICCS correlated well for CD4$^+$ (Fig 2A) and CD8$^+$ T cells (Fig 2B). These data indicate that the IL-10GFP—signal faithfully reports on the IL-10 production of lymphoid cells. However, the GFP-signal from neutrophils (Fig 2C), macrophages (Fig 2D), and Siglec-F$^+$ (Fig 2E) cells was significantly higher than the ICCS-derived signal. Representative dot-plots for all cell types and organs are provided in S3 Fig. Furthermore, the additional staining with a secondary αGFP-AF488-antibody was not able to improve the specificity of the IL-10-signal (S4 Fig). Interestingly, the GFP-signal of monocytes (Fig 2F) and ILCs (Fig 2G) was substantially higher only in the lung tissues, indicating that the increase in the GFP-channel autofluorescence is organ-specific for some cell types.

An overlay of the GFP-signals of CD4$^+$ T cells, CD8$^+$ T cells, neutrophils, macrophages, Siglec-F$^+$ cells, monocytes, and ILCs from control C57BL/6 lung (Fig 3A) and spleen (Fig 3B) indicated that the background GFP-signal was mainly derived from granulocytes. According to the background GFP-signal, cell types ranked as Siglec-F > macrophage > neutrophil > monocyte > ILC. A similar increase in the GFP-channel autofluorescence upon inflammation was noted when alveolar macrophages were analysed (Fig 4).

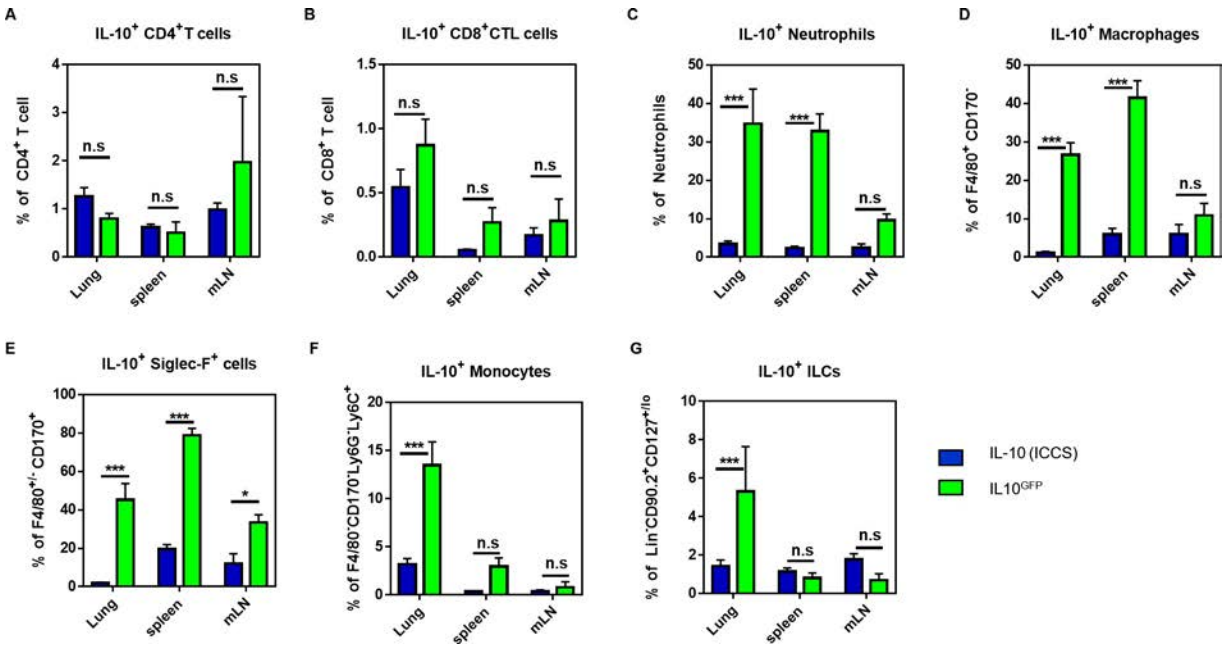

Fig 2. The myeloid-derived IL-10^{GFP} signal is masked by autofluorescence in granulocytes. C57BL/6 and IL-10^{GFP} mice were challenged three times (d0, d1, d2) with either PBS or 10 μg LPS per mouse via aspiration. 16–18 hours after the last administration, the single cell suspension from lungs, spleens, and mLNs were stained for CD4$^+$ T cells (CD45$^+$ CD45R/B220$^-$ CD3ε$^+$ CD4$^+$ CD8α$^-$), CD8$^+$ T cells (CD45$^+$ CD45R/B220$^-$ CD3ε$^+$ CD4$^-$ CD8α$^+$), macrophages (CD45$^+$ CD45R/B220$^-$ CD3ε$^-$ Siglec-F$^-$ F4/80$^+$), Siglec-F$^+$ cells (eosinophils, alveolar macrophages; CD45$^+$ CD45R/B220$^-$ CD3ε$^-$ Siglec-F$^+$ F4/80$^{-/+}$), neutrophils (CD45$^+$ CD45R/B220$^-$ CD3ε$^-$ Siglec-F$^-$ F4/80$^-$ Ly6G$^+$ CD11b$^+$), monocytes (CD45$^+$ CD45R/B220$^-$ CD3ε$^-$ Siglec-F$^-$ F4/80$^-$ Ly6G$^-$ Ly6C$^+$ CD11b$^+$), and ILCs (CD45$^+$ CD45R/B220$^-$ CD3ε$^-$ Siglec-F$^-$ F4/80$^-$ Ly6G$^-$ CD90.2$^+$ CD127$^{lo/-}$). The expression of IL-10 was measured either by GFP$^+$ or by intracellular IL-10 as indicated. **(A-G)** Comparison of the IL-10 signal derived from intracellular cytokine staining (ICCS) or from the GFP-signal (IL10^{GFP}) of IL10^{GFP} mice in (D) CD4$^+$ T cells, (E) CD8$^+$ T cells, (F) neutrophils, (G) macrophages, (H) Siglec-F$^+$ cells (eosinophils, alveolar macrophages), (I) monocytes, and (J) ILCs from indicated organs. The graph shows combined data from two independent experiments (PBS: n = 6 mice/group, LPS: n = 7–9 mice/group in total).

https://doi.org/10.1371/journal.pone.0247895.g002

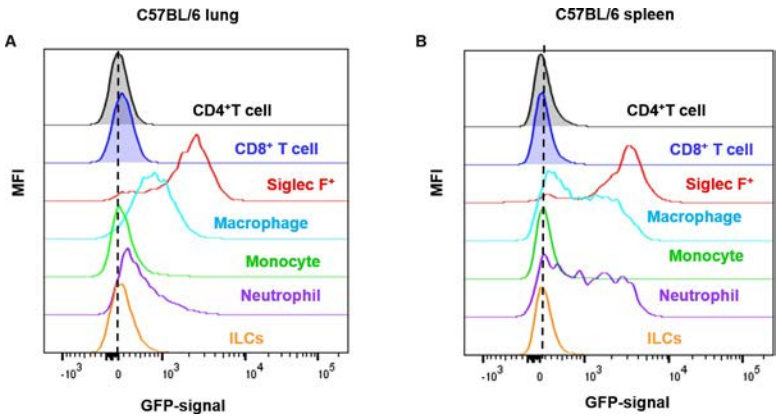

Fig 3. The cell-type-specific autofluorescence in C57BL/6 mice in control conditions. Representative histograms from the **(A)** lung and the **(B)** spleen of PBS challenged C57BL/6 mice, demonstrating the increase in autofluorescence in the GFP-channel for myeloid cells. The graphs show representative data from three independent experiments (PBS: n = 9 mice/group, LPS: n = 13–15 mice/group in total).

https://doi.org/10.1371/journal.pone.0247895.g003

In conclusion, our data indicate that the IL-10^{GFP} (VeRT-X) reporter strain is not suitable to analyse IL-10 production of myeloid cells during inflammation, due to the strong increase in the autofluorescence, which masks the IL-10-specific GFP-signal. Although we only analysed lung, spleen, and mLN of the VeRT-X IL-10^{GFP} reporter strain, it appears likely that this problem will also be relevant to other organs. Importantly, the strong increase of the granulocytic autofluorescence in the GFP-channels was independent of the strain analysed. Therefore, it is expected that other fluorescent reporter lines that utilize the GFP-channel would face similar problems at distinguishing the reporter-specific signal from the autofluorescence signal when analysing granulocytes. Our data indicate that granulocytes are the source of the background GFP-signal, in line with previous publications reporting high levels of autofluorescence [11], although other sources, like collagen deposition [12,13], cannot be excluded. This large increase in false-positive GFP-signals for myeloid cells during inflammation could have been missed previously due to a focus on lymphoid cells or due to a lack of the WT-treated controls. Our data illustrate a general and important technical caveat using GFP-reporter lines

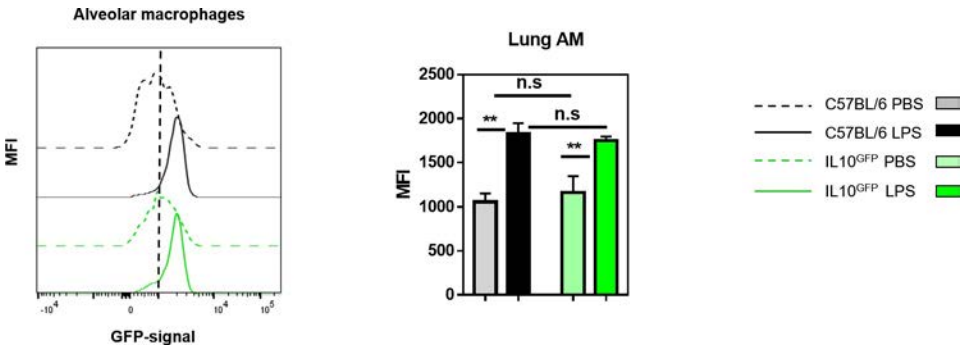

Fig 4. The autofluorescence of alveolar macrophages increases during lung inflammation. C57BL/6 and IL-10^{GFP} mice were subjected to three daily administrations (d0, d1, d2) of 10 μg LPS per mouse via aspiration. 16–18 hours after the last administration, the single-cell suspensions from the lungs were analysed. Representative histogram showing the GFP-signal from alveolar macrophages (CD45$^+$ CD45R/B220$^-$ CD3ε$^-$ Siglec-F$^+$ F4/80$^+$ CD11b$^-$) from C57BL/6 and IL10^{GFP} mice as indicated. The data shown are representative of three independent experiments (PBS: n = 9 mice/group, LPS: n = 13–15 mice/group in total).

https://doi.org/10.1371/journal.pone.0247895.g004

for the analysis of myeloid cells and suggest that previous reports on effector functions of myeloid cells using such GFP-based reporters might require re-evaluation.

Material and methods

Mice

C57BL/6J mice and IL-10^{GFP} (also known as Vert-X) B6(Cg)-Il10$^{tm1.1Karp}$/J mice were originally obtained from Jackson Laboratory (Bar Harbor, USA). All mice were housed in the vivarium of the Izmir Biomedicine and Genome Center (IBG, Izmir, Turkey) in accordance with the respective institutional animal care committee guidelines. All mouse experiments were performed with prior approval by the institutional ethic committee ('Izmir Biomedicine and Genome Center's Ethical Committee on Animal Experimentation'), in accordance with national laws and policies. All the methods were carried out in accordance with the approved guidelines and regulations.

Reagents and monoclonal antibodies

Monoclonal antibodies against the following mouse antigens were used in this study: CD3ε (145.2C11), CD4 (RM4-5), CD8α (53–6.7), CD11b (M1/70), CD11c (N418), CD45 (30-F11), CD45R/B220 (RA3-6B2), CD90.2 (30-H12), CD127 (A7R34), CD170/Siglec-F (E50-2440), F4/80 (BM8), IL-10 (JESS-16E3), Ly6C (HK1.4), Ly6G (1A8). Antibodies were purchased from BD Biosciences (San Diego, USA), BioLegend (San Diego, USA), or ThermoFisher Scientific (Carlsbad, USA). Antibodies were conjugated to Pacific Blue, Brilliant Violet 421, V500, Brilliant Violet 510, Brilliant Violet 570, Brilliant Violet 650, Brilliant Violet 711, Brilliant Violet 785, Brilliant Violet 786, FITC, Alexa Fluor 488, PerCP-Cy5.5, PerCP-eFluor 710, PE, PE-CF594, PE-Cy7, APC, Alexa Fluor 647, Alexa Fluor 700, APC-Cy7, or APC-Fire750. Details on the antibody used in this study are given in the **S1 Table**. Anti-mouse CD16/32 antibody (2.4G2) and Zombie UV Dead Cell Staining Kit were obtained from Tonbo Biosciences (San Diego, USA) and from BioLegend, respectively. Unconjugated mouse and rat IgG antibodies were purchased from Jackson ImmunoResearch (West Grove, USA).

LPS-induced lung inflammation

Lung inflammation was induced by three daily administrations (d0, d1, d2) with 10 μg LPS (#L6386, Sigma-Aldrich, St. Louis, USA) per mouse via pharyngeal/laryngeal aspiration. 16–18 hours after the last challenge, the mice were sacrificed, and lungs, spleens, and mediastinal lymph nodes were collected.

Cell preparation

Lungs were removed and minced into smaller pieces in a 6-well plate (Greiner, Germany). The digestion mixture, composed of 1 mg/mL collagenase D and 0.1 mg/mL DNase I (both from Roche, Switzerland) in complete RPMI medium (Gibco, USA), was added to the samples and incubated for 45 min at 37˚C on a lateral shaker. The lung samples were filtered through 100 μm mesh with PBS, washed twice, and the red blood cells were eliminated by ACK lysis buffer (Lonza, USA). Spleens and mediastinal lymph nodes were homogenized by filtering through a 76 μm mesh with ice-cold PBS (Lonza), washed twice, and red blood cells were eliminated by ACK lysis buffer (Lonza).

In vitro stimulation

Lymphocytes were stimulated *in vitro* with PMA (50 ng/mL) and ionomycin (1 μg/mL) (both Sigma-Aldrich, St. Louis, MO) for four hours at 37˚C in the presence of both Brefeldin A (GolgiPlug) and Monensin (GolgiStop) in complete RPMI medium (RPMI 1640 medium (Life Technologies); supplemented with 10% (v/v) fetal calf serum (FCS), 1% (v/v) Pen-Strep-Glutamine (10.000 U/ml penicillin, 10.000 μg/ml streptomycin, 29.2 mg/ml L-glutamine (Life Technologies)) and 50 μM β-mercaptoethanol (Sigma)). As GolgiPlug and GolgiStop (both BD Biosciences) were used together, half the amount recommended by the manufacturer were used.

Flow cytometry

Flow cytometry was performed as described [14]. In brief, for staining of cell surface molecules, cells were suspended in staining buffer (PBS, 1% BSA, 0.01% NaN_3) and stained with fluorochrome-conjugated antibodies (0.1–1 μg/10^6 cells, or according to the manufacturer's recommendations) for 15 min in a total volume of 50 μl at 4˚C for 30 min. FcεR-blocking antibody αCD16/32 (2.4G2) and unconjugated rat and mouse IgG (Jackson ImmunoResearch) were added to prevent non-specific binding. If biotin-conjugated antibodies were used, cell-bound antibodies were detected with streptavidin conjugates (1:200, or according to the manufacturer's recommendations) in a second incubation step. Dead cells were labelled with a commercially available Zombie UV Dead Cell Staining Kit (BioLegend). For the analysis of intracellular cytokines, cells were fixed and permeabilized with Cytofix/Cytoperm (BD Biosciences) for 10 min at 37˚C. Cells were washed twice and incubated overnight at 4˚C with the fluorochrome-conjugated antibodies and unconjugated rat and mouse IgG in Perm/Wash solution (BD Biosciences), which was followed by additional 5 min incubation in Perm/Wash solution without antibodies. For the analysis of the GFP signal, the cells were fixed with freshly prepared 2% formaldehyde solution for 40 minutes on ice as described [15]. This fixation allows the detection of the GFP-signal together with other intracellular proteins [15]. Then, the cells were permeabilized using the BD Perm/Wash solution. Cells were washed twice and incubated overnight at 4˚C with the fluorochrome-conjugated antibodies and unconjugated rat and mouse IgG in Perm/Wash solution, which was followed by additional 5 min incubation in Perm/Wash solution without antibodies. Cells were analysed with FACSCanto or LSR-Fortessa (BD Biosciences), and data were processed with CellQuest Pro (BD Biosciences) or Flow Jo (Tree Star) software.

Statistical analysis

Data are presented as mean ± standard error of the mean (SEM). The statistical analysis was performed with GraphPad Prism 7.0 software (GraphPad Software, San Diego, USA). One-way ANOVA followed by Holm-Sidak posthoc test are used to compare p-values regarded as $^{*}p\leq0.05$, $^{**}p\leq0.01$, and $^{***}p\leq0.001$.

Supporting information

S1 Fig. Gating strategy to identify leukocytes from the lung, spleen, and mLN. A graphic outline **(A)** and exemplary graphs **(B)** are given to illustrate the gating strategy employed to identify $CD4^+$ T cells ($CD45^+$ $CD45R/B220^-$ $CD3\varepsilon^+$ $CD4^+$ $CD8\alpha^-$ $CD127^{lo}$), $CD8^+$ T cells ($CD45^+$ $CD45R/B220^-$ $CD3\varepsilon^+$ $CD4^-$ $CD8\alpha^+$), macrophages ($CD45^+$ $CD45R/B220^-$ $CD3\varepsilon^-$ Siglec-F^- $F4/80^+$), Siglec-F^+ cells (eosinophils, alveolar macrophages; $CD45^+$ $CD45R/B220^-$ $CD3\varepsilon^-$ Siglec-F^+ $F4/80^{-/+}$), neutrophils ($CD45^+$ $CD45R/B220^-$ $CD3\varepsilon^-$ Siglec-F^- $F4/80^-$ $Ly6G^+$

CD11b^{+}), monocytes (CD45^{+} CD45R/B220^{-} CD3ε^{-} Siglec-F^{-} F4/80^{-} Ly6G^{-} Ly6C^{+} CD11b^{+}), and ILCs in the inflamed lung.
(TIF)

S2 Fig. Efficiency of intracellular IL-10 cytokine staining. Representative flow cytometric dot plots showing the IL-10 staining (ICCS) in splenic CD4^{+} T cells.
(TIF)

S3 Fig. Representative flow cytometry plots for the data presented in Fig 2. C57BL/6 and IL-10^{GFP} mice were challenged three times (d0, d1, d2) with either PBS or 10 μg LPS per mouse via aspiration. 16–18 hours after the last administration, the single cell suspension from **(A)** lungs, **(B)** spleens, and **(C)** mLNs were stained for CD4^{+} T cells (CD45^{+} CD45R/B220^{-} CD3ε^{+} CD4^{+} CD8α^{-}), CD8^{+} T cells (CD45^{+} CD45R/B220^{-} CD3ε^{+} CD4^{-} CD8α^{+}), macrophages (CD45^{+} CD45R/B220^{-} CD3ε^{-} Siglec-F^{-} F4/80^{+}), Siglec-F^{+} cells (eosinophils, alveolar macrophages; CD45^{+} CD45R/B220^{-} CD3ε^{-} Siglec-F^{+} F4/80$^{-/+}$), neutrophils (CD45^{+} CD45R/B220^{-} CD3ε^{-} Siglec-F^{-} F4/80^{-} Ly6G^{+} CD11b^{+}), monocytes (CD45^{+} CD45R/B220^{-} CD3ε^{-} Siglec-F^{-} F4/80^{-} Ly6G^{-} Ly6C^{+} CD11b^{+}), and ILCs (CD45^{+} CD45R/B220^{-} CD3ε^{-} Siglec-F^{-} F4/80^{-} Ly6G^{-} CD90.2^{+} CD127$^{lo/-}$). The expression of IL-10 was measured either by intracellular IL-10 staining (left panel) or GFP—expression (right panel).
(TIF)

S4 Fig. The staining with a secondary αGFP-AF488 antibody does not improve the resolution of the myeloid IL10^{GFP} signal. Representative histograms from the spleen of PBS (left) or LPS (right) challenged C57BL/6 and IL-10^{GFP} mouse, demonstrating the overall GFP-signal detected with or without labelling with secondary αGFP-AF488.
(TIF)

S1 Table.
(TIF)

Author Contributions

Conceptualization: Müge Özkan, Gerhard Wingender.

Data curation: Müge Özkan.

Formal analysis: Müge Özkan, Yusuf Cem Eskiocak.

Funding acquisition: Gerhard Wingender.

Investigation: Müge Özkan, Yusuf Cem Eskiocak, Gerhard Wingender.

Methodology: Müge Özkan, Yusuf Cem Eskiocak, Gerhard Wingender.

Project administration: Müge Özkan, Gerhard Wingender.

Resources: Gerhard Wingender.

Supervision: Gerhard Wingender.

Validation: Müge Özkan.

Visualization: Müge Özkan, Gerhard Wingender.

Writing – original draft: Müge Özkan, Gerhard Wingender.

Writing – review & editing: Müge Özkan, Yusuf Cem Eskiocak, Gerhard Wingender.

References

1. Branchett WJ, Lloyd CM. Regulatory cytokine function in the respiratory tract. Mucosal Immunol [Internet]. 2019 Mar 15; 12(3):589–600. Available from: https://doi.org/10.1038/s41385-019-0158-0 PMID: 30874596
2. Sun J, Madan R, Karp CL, Braciale TJ. Effector T cells control lung inflammation during acute influenza virus infection by producing IL-10. Nat Med. 2009; 15(3):277–84. https://doi.org/10.1038/nm.1929 PMID: 19234462
3. Bracken SJ, Adami AJ, Szczepanek SM, Ehsan M, Natarajan P, Guernsey LA, et al. Long-Term Exposure to House Dust Mite Leads to the Suppression of Allergic Airway Disease Despite Persistent Lung Inflammation. Int Arch Allergy Immunol. 2015; 166(4):243–58. https://doi.org/10.1159/000381058 PMID: 25924733
4. Kawano H, Kayama H, Nakama T, Hashimoto T, Umemoto E, Takeda K. IL-10-producing lung interstitial macrophages prevent neutrophilic asthma. Int Immunol. 2016; 28(10):489–501. https://doi.org/10.1093/intimm/dxw012 PMID: 26976823
5. Sag D, Özkan M, Kronenberg M, Wingender G. Improved Detection of Cytokines Produced by Invariant NKT Cells. Sci Rep. 2017; 7(1). https://doi.org/10.1038/s41598-017-16832-1 PMID: 29192280
6. Bouabe H. Cytokine Reporter Mice: The Special Case of IL-10. Scand J Immunol [Internet]. 2012 Jun; 75(6):553–67. Available from: http://doi.wiley.com/10.1111/j.1365-3083.2012.02695.x. PMID: 22429026
7. Madan R, Demircik F, Surianarayanan S, Allen JL, Divanovic S, Trompette A, et al. Nonredundant Roles for B Cell-Derived IL-10 in Immune Counter-Regulation. J Immunol. 2009; 183(4):2312–20. https://doi.org/10.4049/jimmunol.0900185 PMID: 19620304
8. Mitchell AJ, Pradel LC, Chasson L, Van Rooijen N, Grau GE, Hunt NH, et al. Technical Advance: Autofluorescence as a tool for myeloid cell analysis. J Leukoc Biol [Internet]. 2010 Sep; 88(3):597–603. Available from: http://doi.wiley.com/10.1189/jlb.0310184. PMID: 20534703
9. Telford WG, Hawley T, Subach F, Verkhusha V, Hawley RG. Flow cytometry of fluorescent proteins. Methods [Internet]. 2012; 57(3):318–30. Available from: https://doi.org/10.1016/j.ymeth.2012.01.003 PMID: 22293036
10. Peñaloza HF, Noguera LP, Ahn D, Vallejos OP, Castellanos RM, Vazquez Y, et al. Interleukin-10 produced by Myeloid-Derived suppressor cells provides protection to Carbapenem-Resistant klebsiella pneumoniae sequence type 258 by enhancing its clearance in the airways. Infect Immun. 2019; 87(5). https://doi.org/10.1128/IAI.00665-18 PMID: 30804104
11. Tighe RM, Misharin A V., Jakubzick C V., Brinkman R, Curtis JL, Duggan R, et al. Improving the quality and reproducibility of flow cytometry in the lung. Am J Respir Cell Mol Biol. 2019; 61(2):150–61. https://doi.org/10.1165/rcmb.2019-0191ST PMID: 31368812
12. Black PN, Ching PST, Beaumont B, Ranasinghe S, Taylor G, Merrilees MJ. Changes in elastic fibres in the small airways and alveoli in COPD. Eur Respir J. 2008; 31(5):998–1004. https://doi.org/10.1183/09031936.00017207 PMID: 18216063
13. Kretschmer S, Pieper M, Hüttmann G, Bölke T, Wollenberg B, Marsh LM, et al. Autofluorescence multiphoton microscopy for visualization of tissue morphology and cellular dynamics in murine and human airways. Lab Investig. 2016; 96(8):918–31. https://doi.org/10.1038/labinvest.2016.69 PMID: 27400364
14. Wingender G, Birkholz a. M, Sag D, Farber E, Chitale S, Howell a. R, et al. Selective Conditions Are Required for the Induction of Invariant NKT Cell Hyporesponsiveness by Antigenic Stimulation. J Immunol [Internet]. 2015; 195(8):3838–48. Available from: http://www.jimmunol.org/cgi/doi/10.4049/jimmunol.1500203. PMID: 26355152
15. Heinen P, Wanke F, Moos S, Attig S, Waisman A, Kurschus FC, et al. Improved Method to Retain Cytosolic Reporter Protein Fluorescence While Staining for Nuclear Proteins. 2014;(3). https://doi.org/10.1002/cyto.a.22451 PMID: 24616430

Antibody	conjugate	clone	host	catalog number	company	dilution factor
CD11b	BV650	M1/70	Rat	101259	BioLegend	1:200
CD11b	PerCP-Cy5.5	M1/70	Rat	101228	BioLegend	1:1000
CD127	APC-Cy7	A7R34	Rat	135040	Biolegend	1:200
CD127	BV510	A7R34	Rat	135033	Biolegend	1:200
CD127	BV650	A7R34	Rat	135043	Biolegend	1:100
CD170 / Siglec F	PE-CF594	E50-2440	Rat	562757	BD Biosciences	1:400
CD3ε	BUV395	145-2C11	Armenian Hamster	563565	BD Biosciences	1:100
CD4	AF700	RM4-5	Rat	100536	Biolegend	1:800
CD45	V500	30-F11	Rat	561487	BD Biosciences	1:400
CD45	BV605	30-F11	Rat	103139	Biolegend	1:400
CD45R	AF647	RA3-6B2	Rat	557683	BD Biosciences	1:400
CD45R / B220	BV650	RA3-6B2	Rat	563893	BD Biosciences	1:200
CD45R / B220	PE-Cy7	RA3-6B2	Rat	25-0452-82	ThermoFisher/eBio	1:400
CD8α	BV650	53-6.7	Rat	100741	Biolegend	1:200
CD8α	BV711	53-6.7	Rat	100748	Biolegend	1:400
CD90.2 / Thy1.2	BV570	30-H12	Rat	105329	BioLegend	1:200
F4/80	PE	BM8	Rat	123110	BioLegend	1:800
IL-10	APC	JES5-16E3	Rat	505010	BioLegend	1:100
Ly6G	BV421	1A8	Rat	127628	Biolegend	1:400
Ly6G	BUV395	1A8	Rat	563978	BD Biosciences	1:200
Ly6G	PE-Cy7	1A8	Rat	127618	BioLegend	1:400
MHC II (I-A/I-E)	Pacific Blue	M5/114.15.2	Rat	107620	BioLegend	1:400
MHC II (I-A/I-E)	APC-Fire750	M5/114.15.2	Rat	107652	BioLegend	1:1000

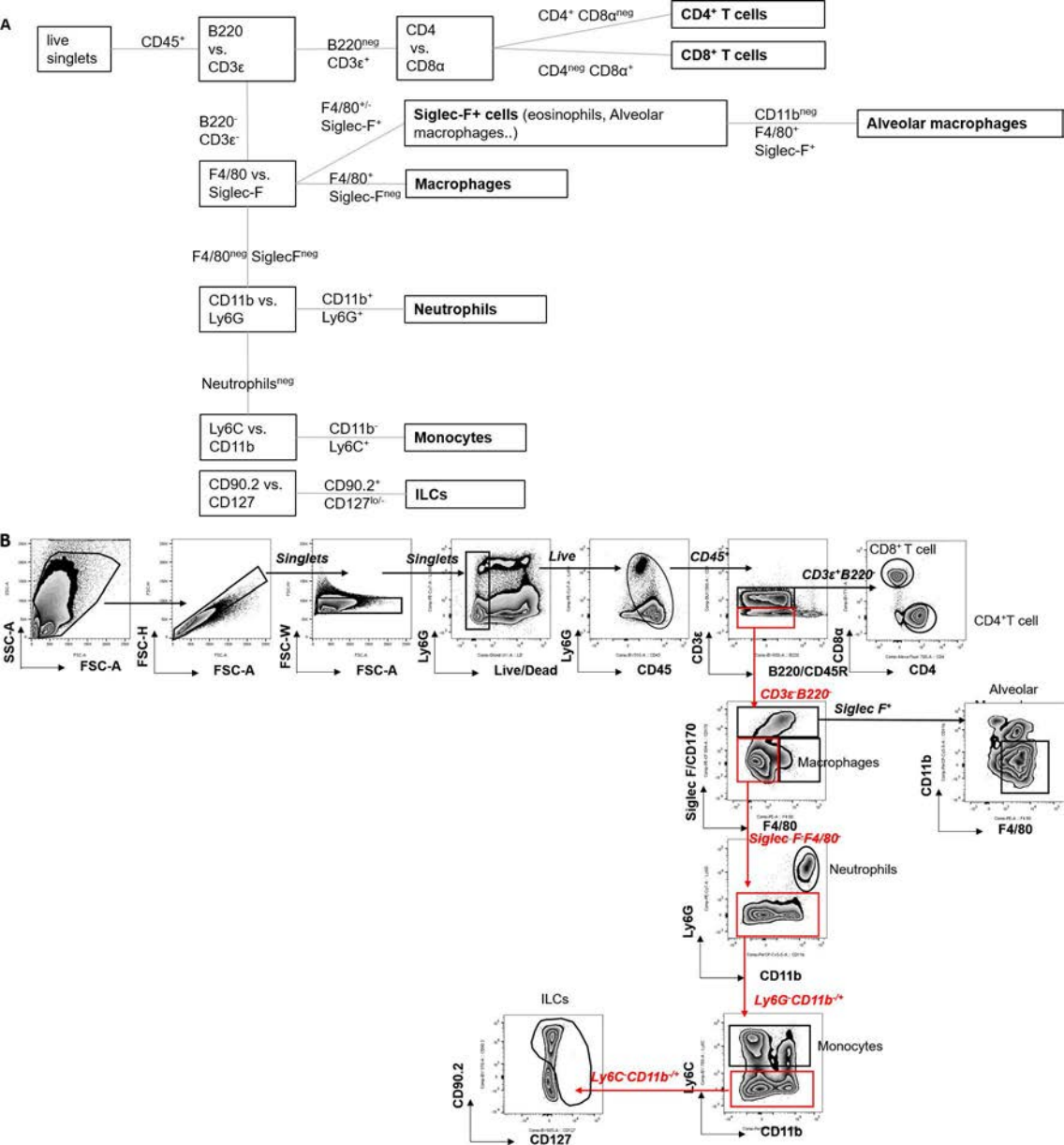
A
live singlets
CD45+
B220 vs. CD3ε
B220neg CD3ε+
CD4 vs. CD8α
CD4+ CD8αneg
CD4+ T cells
CD4neg CD8α+
CD8+ T cells
B220- CD3ε-
F4/80+/- Siglec-F+
Siglec-F+ cells (eosinophils, Alveolar macrophages..)
CD11bneg F4/80+ Siglec-F+
Alveolar macrophages
F4/80 vs. Siglec-F
F4/80+ Siglec-Fneg
Macrophages
F4/80neg SiglecFneg
CD11b vs. Ly6G
CD11b+ Ly6G+
Neutrophils
Neutrophilsneg
Ly6C vs. CD11b
CD11b- Ly6C+
Monocytes
CD90.2 vs. CD127
CD90.2+ CD127lo/-
ILCs
B
SSC-A
FSC-A
FSC-H
FSC-A
Singlets
FSC-W
FSC-A
Singlets
Ly6G
Live/Dead
Live
Ly6G
CD45
CD45+
CD3ε
B220/CD45R
CD3ε+B220-
CD8α
CD4
CD8+ T cell
CD4+T cell
CD3ε-B220-
Siglec F+
Alveolar
Siglec F/CD170
Macrophages
F4/80
CD11b
F4/80
Siglec F-F4/80-
Neutrophils
Ly6G
CD11b
Ly6G-CD11b-/+
ILCs
Monocytes
CD90.2
Ly6C-CD11b-/+
Ly6C
CD127
CD11b

Gated on CD45$^+$ CD45R/B220$^-$ CD3e$^+$ CD4$^+$

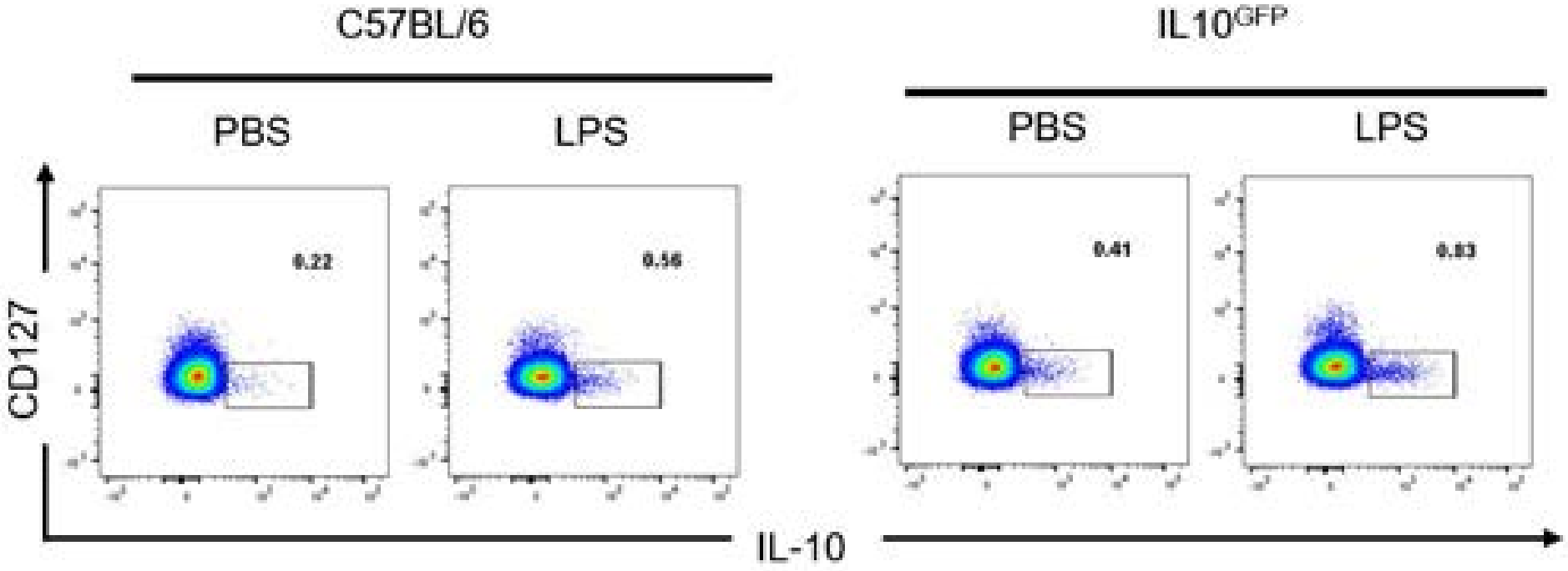

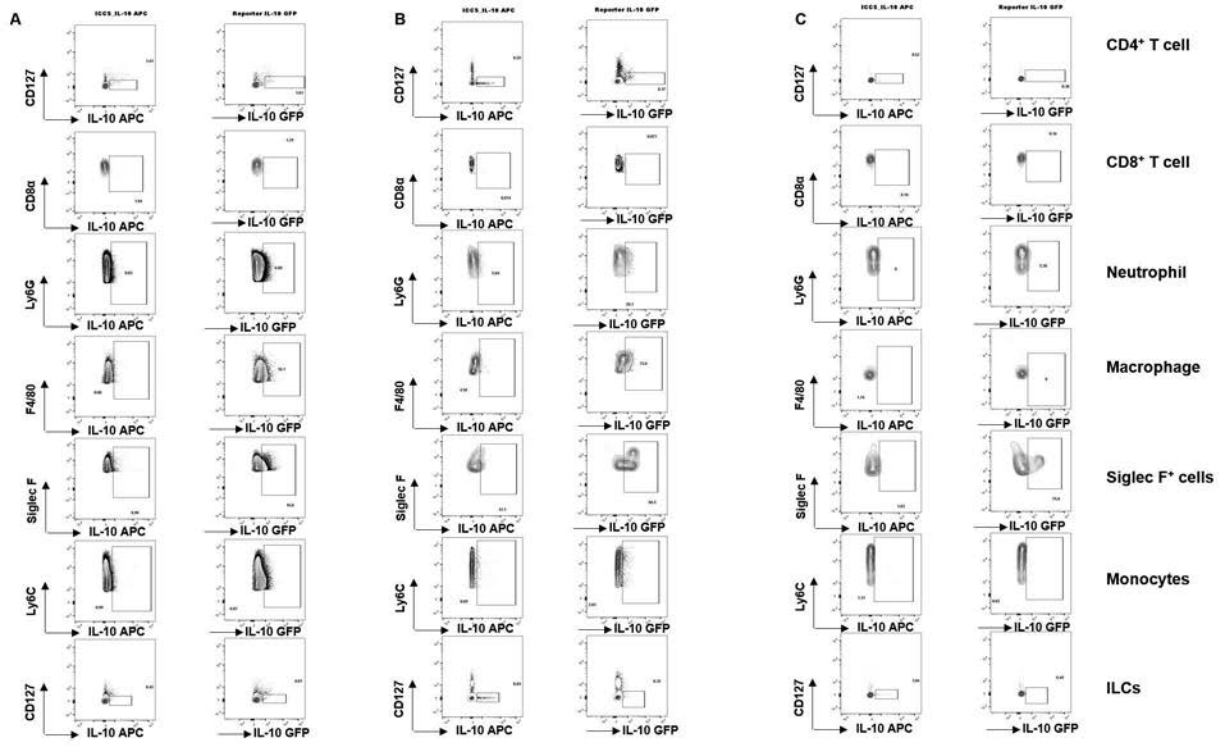
A
B
C
CD127
CD8α
Ly6G
F4/80
Siglec F
Ly6C
CD127
IL-10 APC
IL-10 GFP
CD4⁺ T cell
CD8⁺ T cell
Neutrophil
Macrophage
Siglec F⁺ cells
Monocytes
ILCs

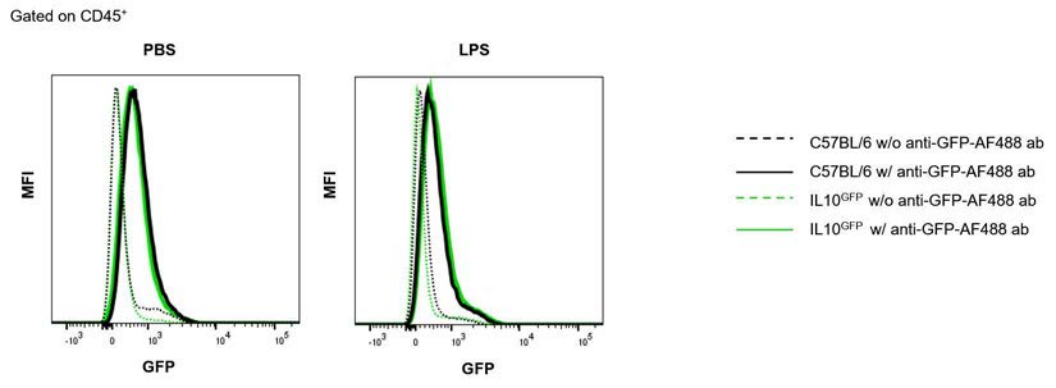
Gated on CD45+
PBS
LPS
MFI
MFI
GFP
GFP
C57BL/6 w/o anti-GFP-AF488 ab
C57BL/6 w/ anti-GFP-AF488 ab
IL10GFP w/o anti-GFP-AF488 ab
IL10GFP w/ anti-GFP-AF488 ab